CHAPTER IV
RESULTS AND DISCUSSION

4.1 Characterization of Monooxazine Benzoxazine Derivatives

In the previous work, Yoswathananont (1999), concluded that benzoxazine monomer can be coupled onto silica by using the aminopropyl triethoxysilane instead of amine derivatives. Here, it can be expected that the silane coupling group can be introduced onto the dimer at either aza methylene or the oxazine position. The preliminary studies indicated that the silane coupling agent could not be introduced by the reaction of benzoxazine monomer with aminoalkylethoxysilane. The unsuccessful of the reaction might come from the bulky group of the aminoalkyltriethoxysilane which prevents the ease of ring opening reaction.

Laobuthee *et al.* (in preparation), reported that benzoxazine dimers reacted with formaldehyde and amine to perform another step of the Mannich reaction. The resulting dimer showed the asymetric structure and is monooxazine benzoxazine derivatives as confirmed by ^{1}H-NMR, EA and FTIR. In that case, the benzoxazine dimer with a monooxazine ring still maintained its intramolecular hydrogen bonding as suggested from the FTIR and NMR.

Based on this model reaction, benzoxazine dimer was applied as a starting material to process Mannich reaction by using aminopropyl triethoxysilane as a primary amine. In the present work, we used benzoxazine dimer **1** which has cyclohexyl amine at the aza group to react with silane

coupling agent, followed by the coupling onto fumed silica to obtain final product, as shown in Scheme 3.2 (see page 13).

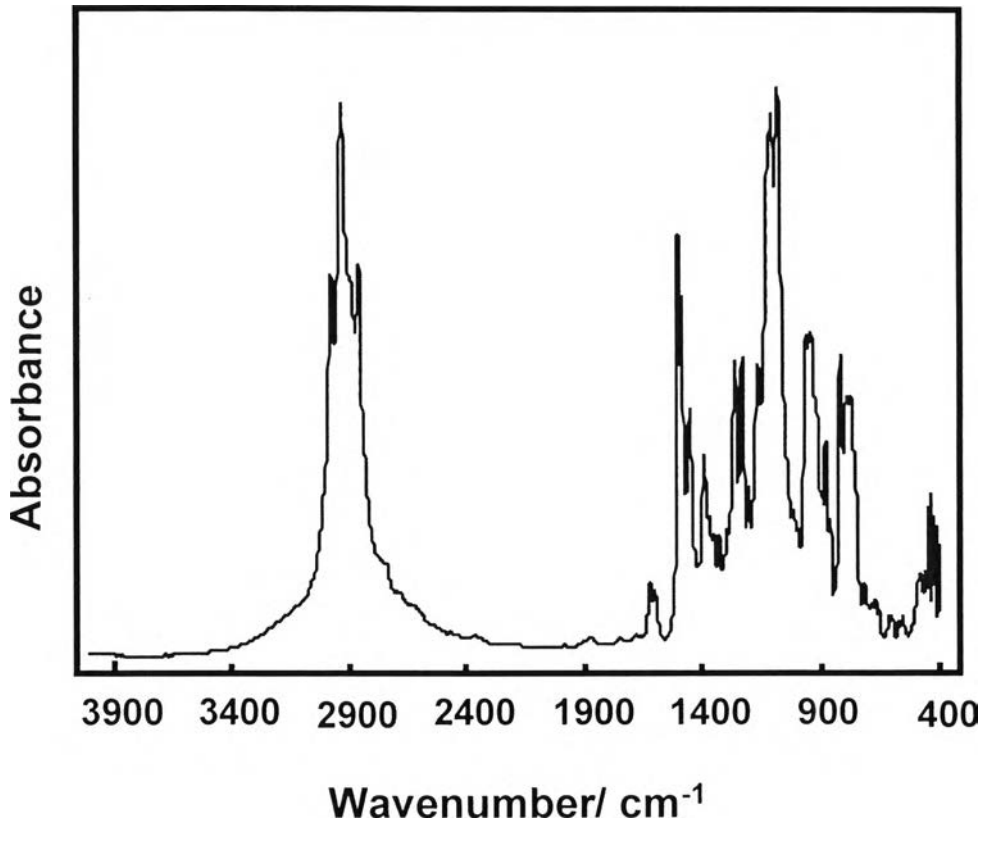

Figure 4.1. FTIR spectrum of **2**.

FTIR spectrum of **2** (Figure 4.1) shows the intramolecular hydrogen bonding observed from the broad peak from 3100 ~ 3300 cm^{-1}, and the oxazine peak at 1503 cm^{-1}. The open ring structure could be confirmed from 1498 cm^{-1}, which is belong to -C-N-. The silane group was also confirmed from the sharp peak of 1104~1080 cm^{-1} assigned to Si-O-C and 916 cm^{-1} for $Si\text{-}OC_2H_5$.

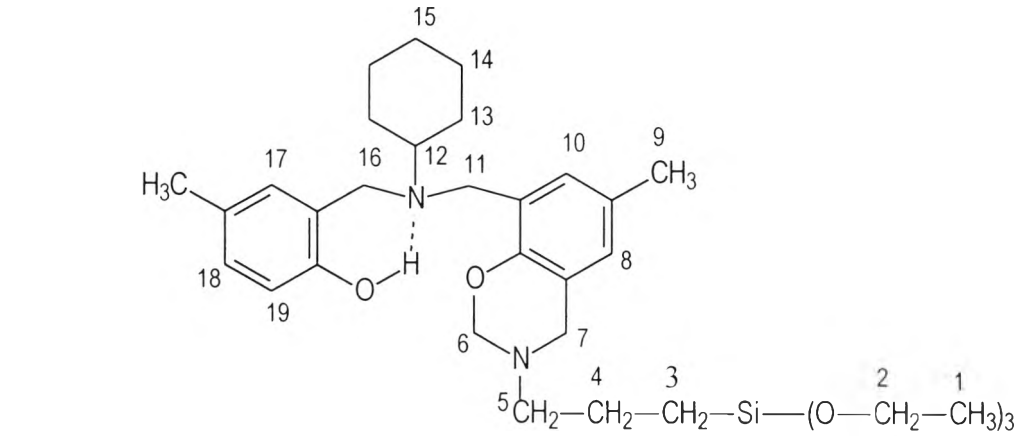

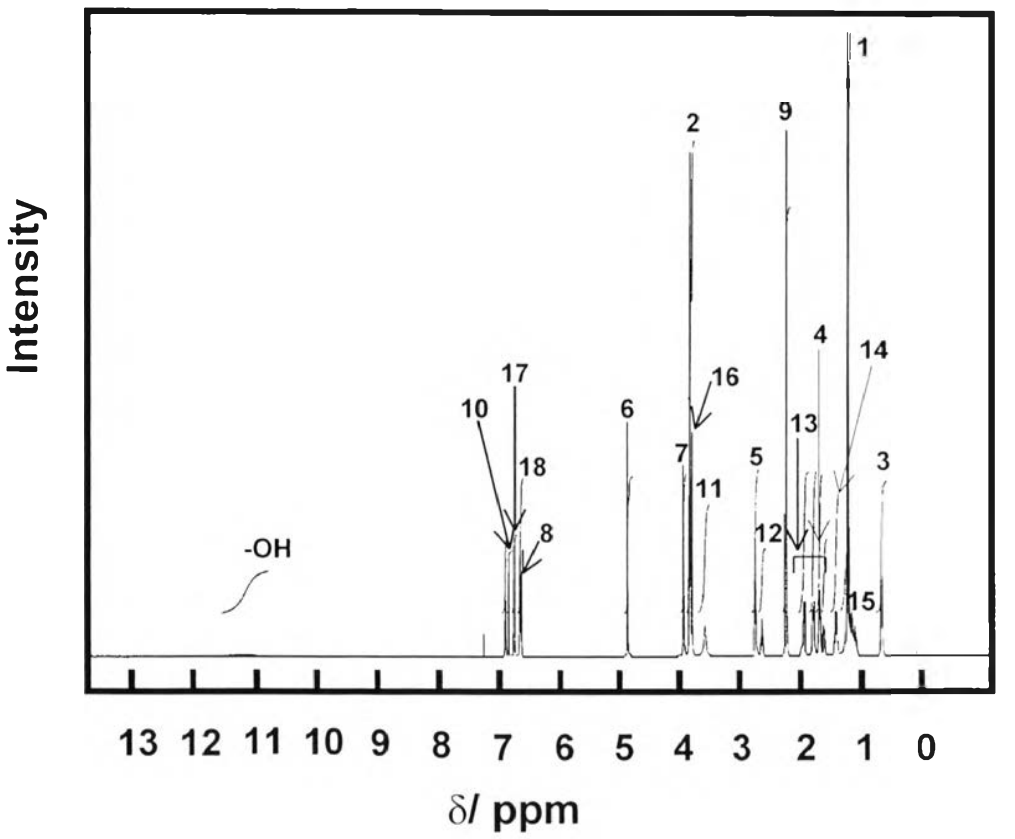

Figure 4.2 ^{1}H-NMR spectrum of **2**.

The success of the reaction was further confirmed by ^{1}H-NMR and NOESY ^{1}H-NMR. The peak assignment of ^{1}H-NMR is shown in Figure 4.2 and summarized in Table 4.1.

Table 4.1 ^{1}H-NMR Chemical Shifts of **2** in $CDCl_3$ at 25°C

Peak Number	Chemical Shift (ppm)
1	1.21 (t)
2	3.83 (q)
3	0.68 (t)
4	3.78 (m)
5	2.78 (t)
6	4.87 (s)
7	3.93 (s)
8	6.63 (s)
9	2.21 (s)
10	6.83 (s)
11	3.60 (s)
12	2.62 (t)
13	1.61-1.98 (t, d)
14	1.20 (m)
15	1.10 (m)
16	3.79 (s)
17	6.78 (s)
18	6.63 (d)
19	6.92 (d)

The dimer structure could be confirmed from the methylene linkage observed at δ 3.60, and 3.79 as singlet peaks. The monooxazine ring is clarified from the singlet peaks at δ 3.93, and 4.87, which are referred to two methylene groups of oxazine ring. Meanwhile, the OH peak is found at the broad peak δ 11.20. The coupling of silylethoxy group can be confirmed from N-C**H**$_2$-CH$_2$-CH$_2$ at δ 2.78 (triplet), N-CH$_2$-C**H**$_2$-CH$_2$ at δ 3.78 (multiplet), and N-CH$_2$-CH$_2$-C**H**$_2$-Si at δ 0.68 (triplet). The ethoxy protons are identified at δ 1.21 (triplet) and δ 3.83 (quartet) for methyl and methylene, respectively.

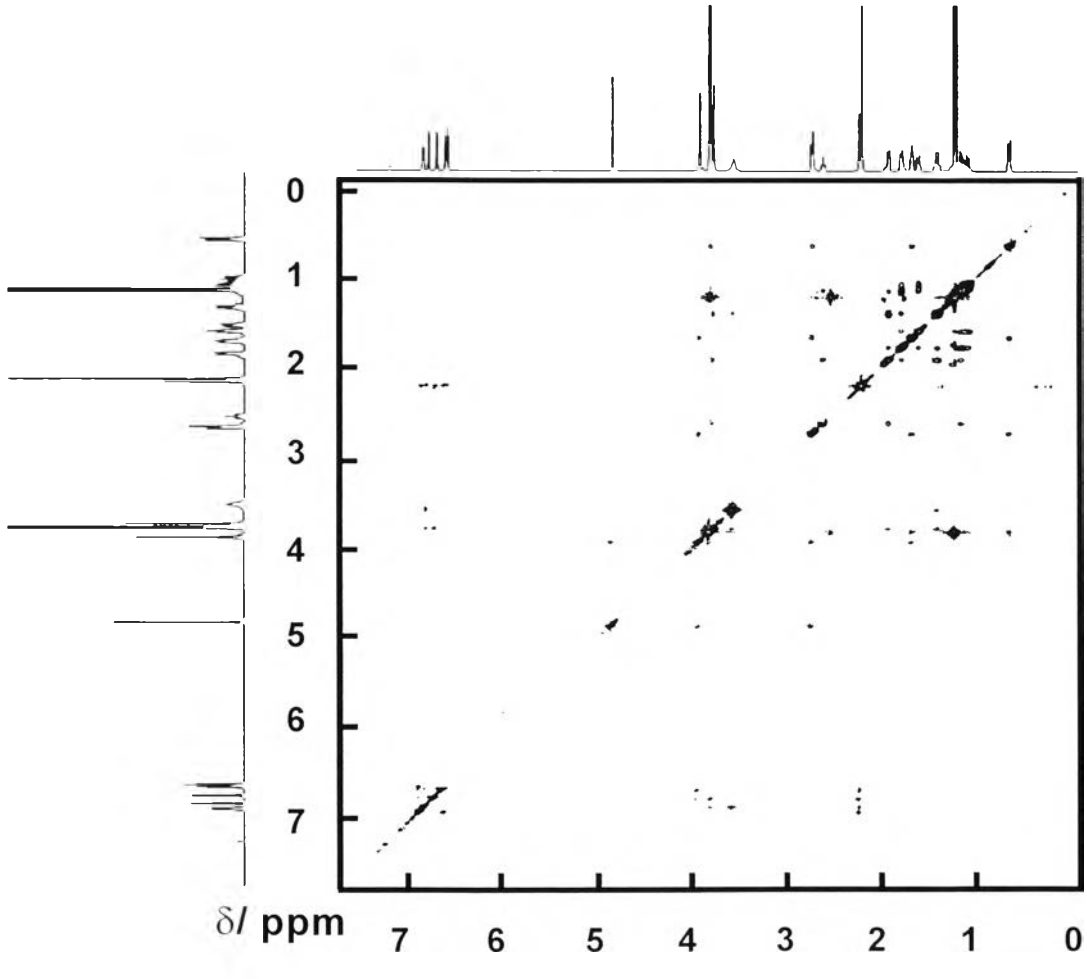

Figure 4.3 NOESY ^{1}H-NMR spectrum of **2**.

We applied 2D-NMR to confirm the monooxazine benzoxazine dimer or the compound **2** (Figure 4.3). It should be noted that if the monooxazine structure existed, there should be interaction between N-C**H**$_2$-CH$_2$-CH$_2$ and both methylene in oxazine ring. The related correlation peaks are summarized in Table 4.2.

Table 4.2. NOESY ^{1}H-NMR of **2** in $CDCl_3$ at 25^{o}C

Proton Number	Correlation Proton
1	4, 13, 12, 5, 2, 16, 19, 10, 3
2	4, 17, 10, 4, 1, 3
3	4, 5, 2
4	3, 1, 5, 2, 7
5	6, 7, 4, 3, 2
6	7, 5, 4, 2, 3
7	6, 5, 4, 8, 17, 3
8	7, 9, 10
9	8, 18, 17, 10, 19, 4
10	8, 16, 11, 9
11	10, 16, 14, 16, 13
12	13, 15
13	12, 16, 14, 15
14	13, 12, 11, 16
15	12, 14, 13, 16
16	17, 10, 12, 13, 14, 15, 4
17	16, 9, 8, 18, 10, 19
18	19, 16, 9, 6, 7
19	18, 9, 10, 17, 8, 9

4.2 Coupling Ratio of 2 onto Fumed Silica

The coupling reaction of **2** onto silica was achieved by refluxing in xylene under nitrogen atmosphere for 24 h. The product was studied by DRIFT FT-IR peak subtraction technique and found the peak of Si-O-Si at 1030 cm^{-1} (Figure 4.4). The obtained silica resin was confirmed to be coupled with **2** by the peak at 1503 cm^{-1} assigned to oxazine ring and at 1489 cm^{-1} due to open ring of dimer structure.

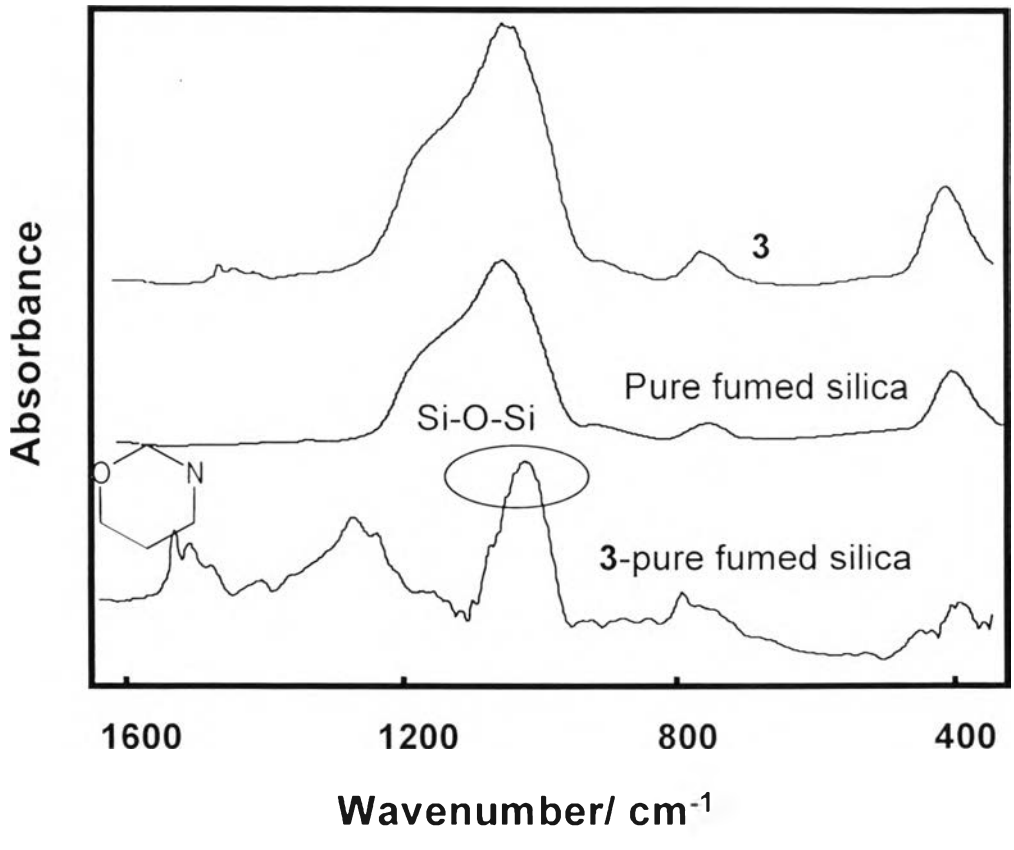

Figure 4.4 DRIFT FTIR spectrum of **3**; pure fumed silica; and **3**-pure fumed silica.

It should be noted that even at reflux temperature of xylene in the reaction, the oxazine ring still remained and **2** was stable enough to be coupled onto the silica surface to obtain **3**.

Scheme 4.1 Patterns of compound **3** and the calculated %C, H, and N

Pattern 1

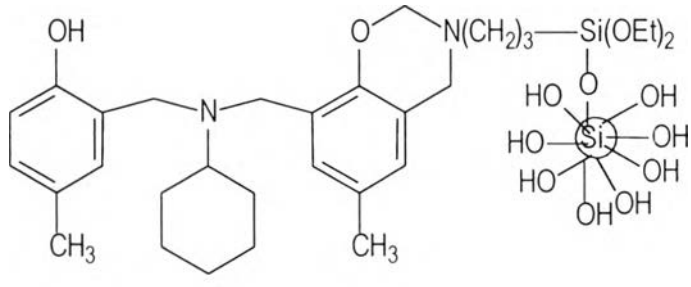

$(C_{31}H_{47}O_4N_2Si)\ (SiO)\ (SiOH)_{x-1}$

Cald.%C, 27.16; %H, 3.87, %N, 1.92 (x=20)

Pattern 2

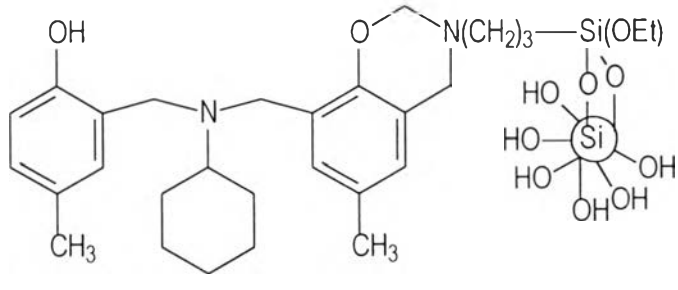

$(C_{29}H_{42}O_3N_2Si)\ (SiO)_2\ (SiOH)_{x-2}$

Cald. %C,27.56, % H, 3.62; %N, 1.95 (x= 21)

Pattern 3

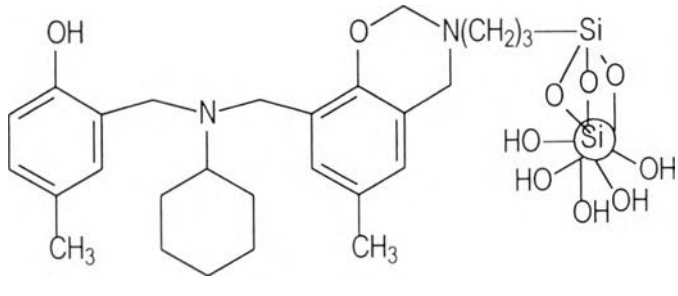

$(C_{27}H_{37}O_2N_2Si)\ (SiO)_3\ (SiOH)_{x-3}$

Cald. %C,27.56, % H, 3.62; %N, 1.95 (x= 23)

The coupling of **2** onto pure fumed silica was considered for % C, H, and N under various assumptions as summarized in Scheme 4.1 i.e., three main patterns based on ethoxy elimination.

Referring to the elemental analysis, it was found that %C = 21.80, %H= 2.70, and %N= 1.92, while the calculated data can be verified depending upon the patterns and the fraction of SiOH. However, since the coupling reaction leads to many patterns of chemical structures, as shown in Scheme 4.1. The amount of N calculated in each pattern is constant, which is approximately 1.92. Thus, the ratio of SiOH and monooxazine benzoxazine dimer was around 20 ~ 22:1 to satisfy the found value of %N in EA.

4.3 Ion Interaction Ability of 2

In order to evaluate the ion extraction ability of **3**, it is important to clarify **2** on the ion interaction ability. Techakamolsuk reported that benzoxazine dimers act as a host compound and show ion interaction ability. In this case, compound **1** was modified to compound **2**, which was different from **1** owing to the oxazine ring. Compound **2** was studied on the ion interaction ability with a series of transition metal.

The equilibrium time for ion interaction of **2** was studied by using $MnCl_2$. As shown in Figure 4.5, after the ion aqueous solution was mixed with organic phase of **2** and left for 15 minutes, the ion extraction reached the maximum % extraction. Thus, the ion interaction time was operated for 15 minutes. It could be concluded that **2** acted as a host compound to interact with transition metal ions.

It should be noted that the ion interaction was achieved by using the lone pair electrons of nitrogen and oxygen. Thus, pH value should show the

effect on the ion interaction between **2** and transition metal ions. The effect of concentration **2** on the ion extraction ability was studied.

Figure 4.6 clarifies that at higher concentration, the % extraction was significant. Considering the result, we used the concentration 0.1 mol/L for every extraction.

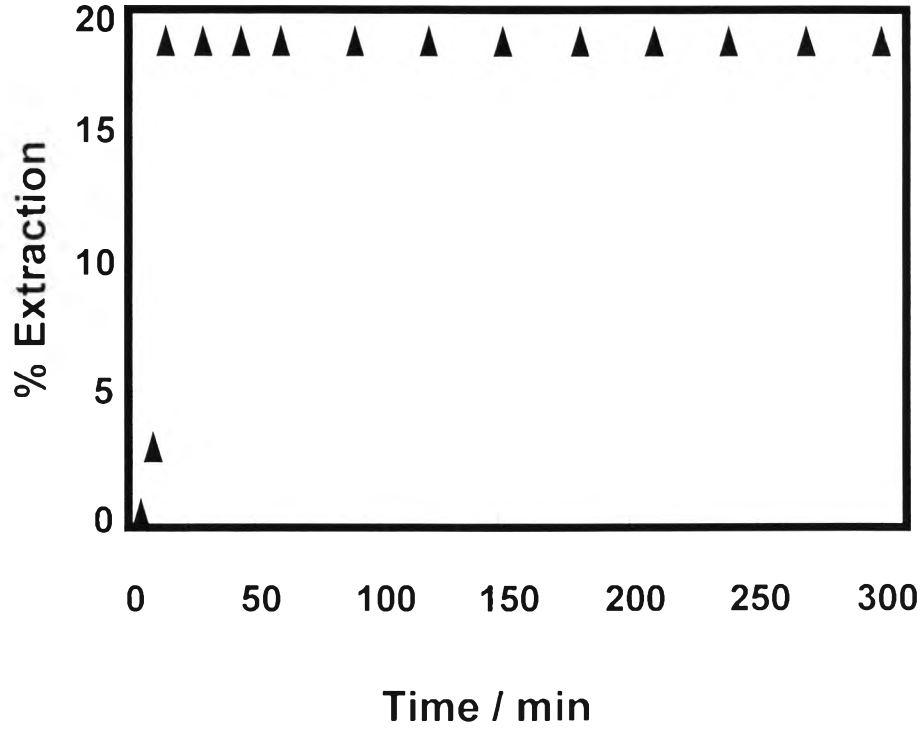

Figure 4.5 Equilibrium time for interaction of **2** with Mn^{2+}.

Figure 4.7 shows that the % extraction is controlled by pH. For all tested transition metals, when the pH value was increased (above 7), % extraction increased. Here, Pb^{2+} was the most extracted while Mn^{2+} was the least extracted species for all pH values. In the case of basic condition, the transition metal ion might precipitate with hydroxide ion existed as a salt in the buffer solution. Thus, the apparent % extraction was higher than the real situation. In order to confirm this, K_{SP} (Solubility Product Constant) value of the metal species in the system has to be determined. However, since the

the metal species in the system has to be determined. However, since the metal ion concentration in the system was very low (10^{-4} M), we did not observe the precipitation obviously in the preparation step of metal salt in buffer solution. The pH effect was explained as shown in schematic draw (Scheme 4.2).

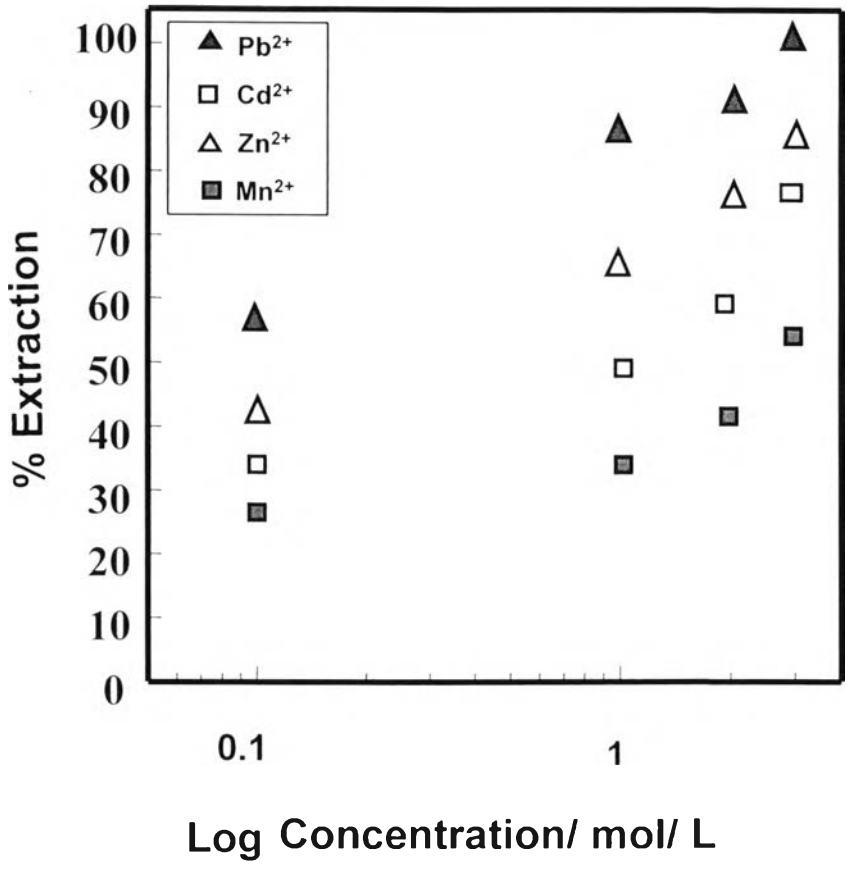

Figure 4.6 Percent extraction of **2** in various concentration.

The ion interaction was low in acid condition, which might be derived from the fact that the oxygen and nitrogen atoms were protonated. However, in the neutral condition, the ion interaction can be achieved efficiently by using lone pair electrons of oxygen and nitrogen atoms.

The ion selectivity might come as a result of space for metal provided by the host and/or the host-guest interaction occurring between lone pair

the tested ions are in the order of $Pb^{2+} > Cd^{2+} > Zn^{2+} > Mn^{2+}$. The result was corresponded to the size order. In another words, Mn^{2+} might be too small to be entrapped by **2**.

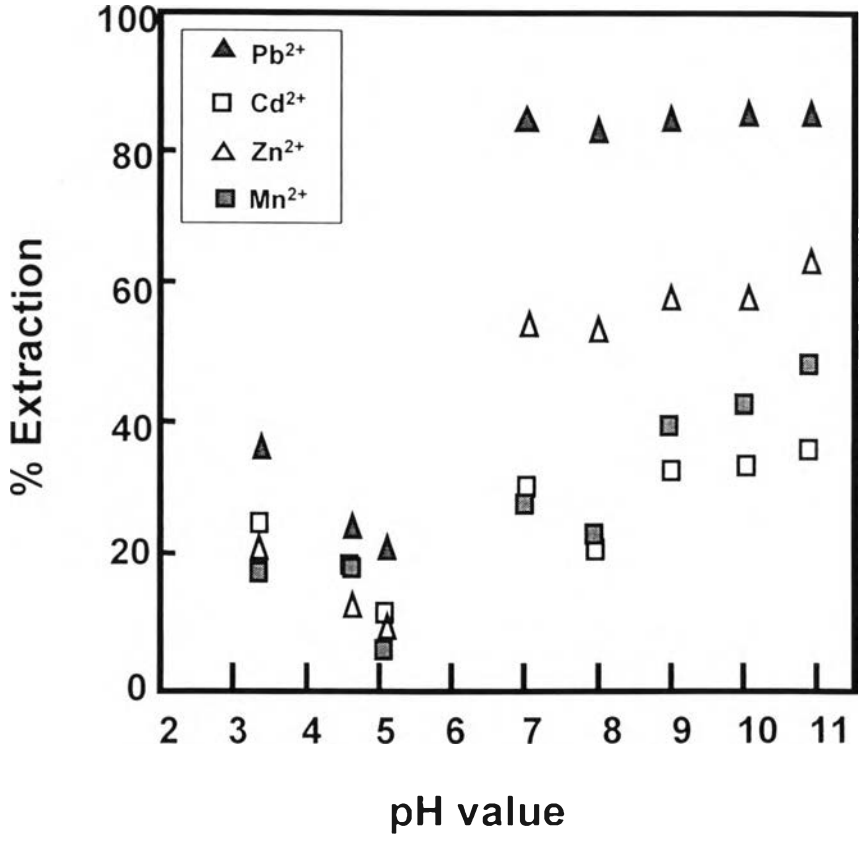

Figure 4.7 Percent extraction in various pH values.

Taking the valence electron into consideration, in the case of Pb which has the valence electron of $5d^{10}\ 6s^2$, the complex formation would be stabilized as a coordinative covalent bond between oxygen atom of **2** and Pb^{2+}. In this case Pb^{2+} would change the valence electron to $5d^{10}\ 6s^0$. As a result, the complexation between Pb^{2+} was significant as compared to other metals.

Scheme 4.2 Schematic draw of ion interaction of **2** in: a) acidic, b) neutral, and c) basic condition

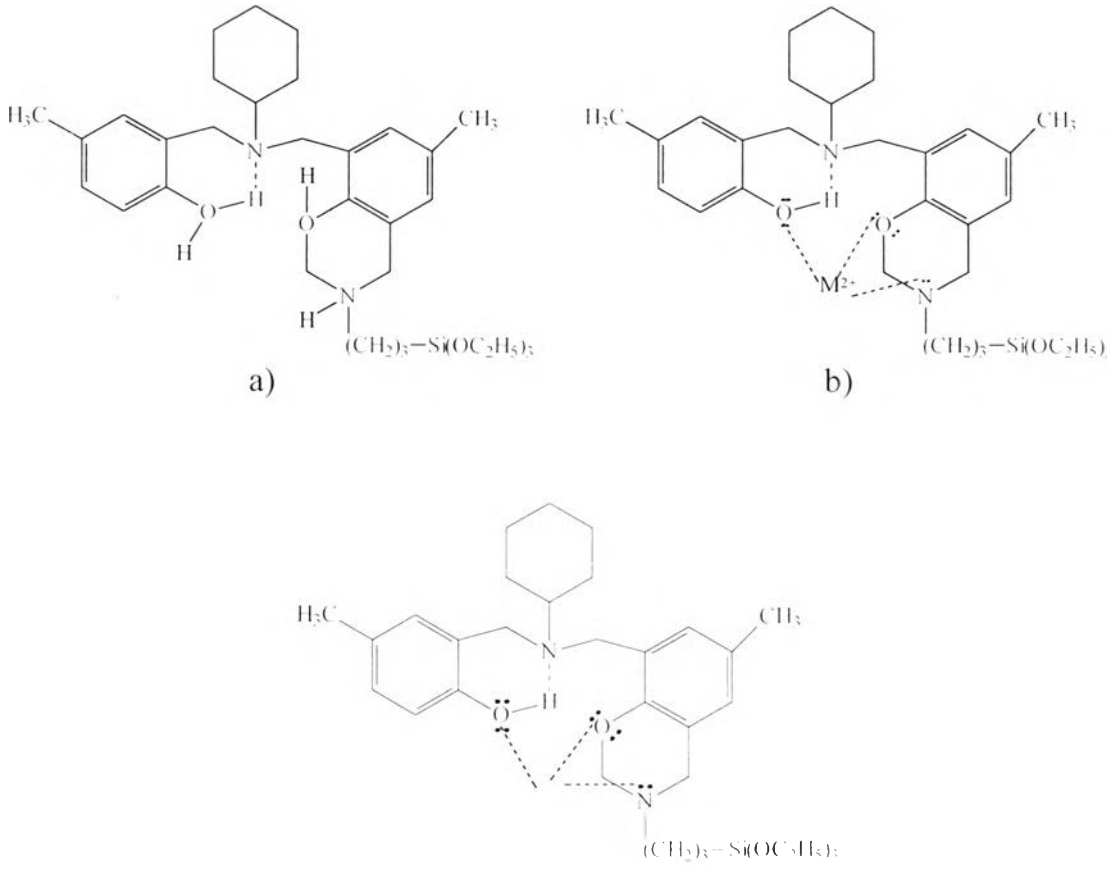

4.3 Ion Extraction Ability of Resin 3

Resin **3** was applied as an ion extraction material. In the present case, the host-guest properties of **2** were applied to extract transition metal ion by using interaction at molecular level or so-called host guest properties. As shown in Figure 4.9, the ion extraction ability was studied as compared to that of pure silica. In the case of silica, the % extraction of ions can not be detected.

However, in the case of basic condition, it should be noticed that even at high pH, the % extraction was not observed. In the previous section (see Ion Interaction Ability of **2**), it was discussed that the metal salts could be precipitated in high pH due to the K_{sp} value, however, if the metal should be precipitated, % extraction of ions by using pure silica must show some high level of % extraction. Figure 4.8 shows that there is no % extraction occurred in basic condition, thus, it can be concluded that the % extraction in basic condition operated in the present work was not affected from the metal salt precipitation.

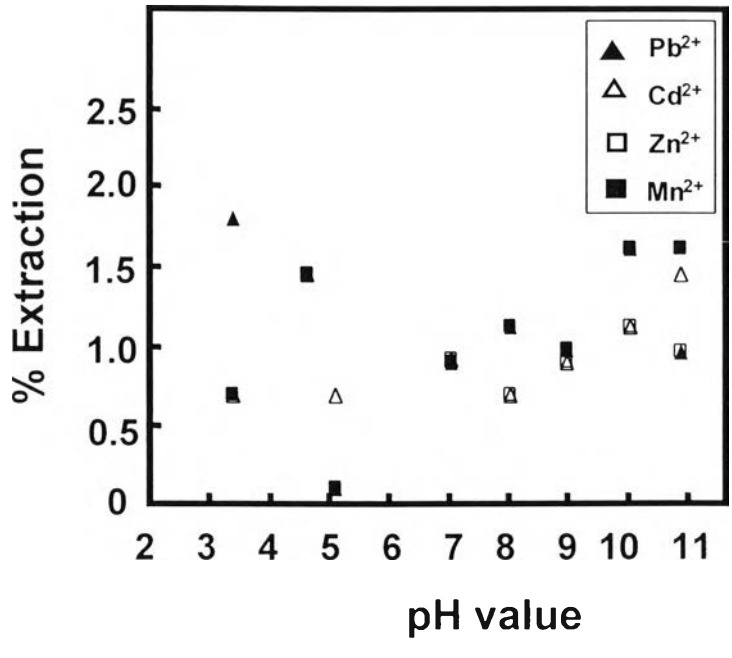

Figure 4.8 Percent extraction of pure fumed silica in various pH values.

Figure 4.9 demonstrates the % extraction of resin **3** related to the pH value. In the acid condition, only slightly % extraction could be found, however, in the neutral and basic condition, the % extraction was significant. The ion extraction selectivity was observed as $Pb^{2+} > Cd^{2+} \sim Zn^{2+} \sim Mn^{2+}$,

which was resemble to the case of **2**. However, the % extraction was lower than that of **2**. This reflected the coupled amount **2** onto silica surface.

Considering the ion extraction using **2** and **3**, it was found that with the same metal ion concentration, **2** showed higher %extraction than **3** for 50%. In order to evaluate the difference of ion extraction ability between **2** and **3**, the amount of **2** coupling on **3** was evaluated. The amount of **2** could be evaluated as follows: Assume that **3** has the formula structure as pattern 1 in Scheme 4.2, thus, the amount of resin used (0.05 g) could be calculated for the effective host **2** to be only 3.4×10^{-5} mol. However, in the case of **2** used in the experiment (Figure 4.6), the concentration was 0.1 M or 5.0×10^{-4} mol. Thus, it can be mentioned that **3** showed less activity (Figure 4.9) as compared to that of **2** (Figure 4.7) because **3** has host **2** on the surface only 3.4×10^{-5} mol or about 14 times less than the case of **2** used in Figure 4.6.

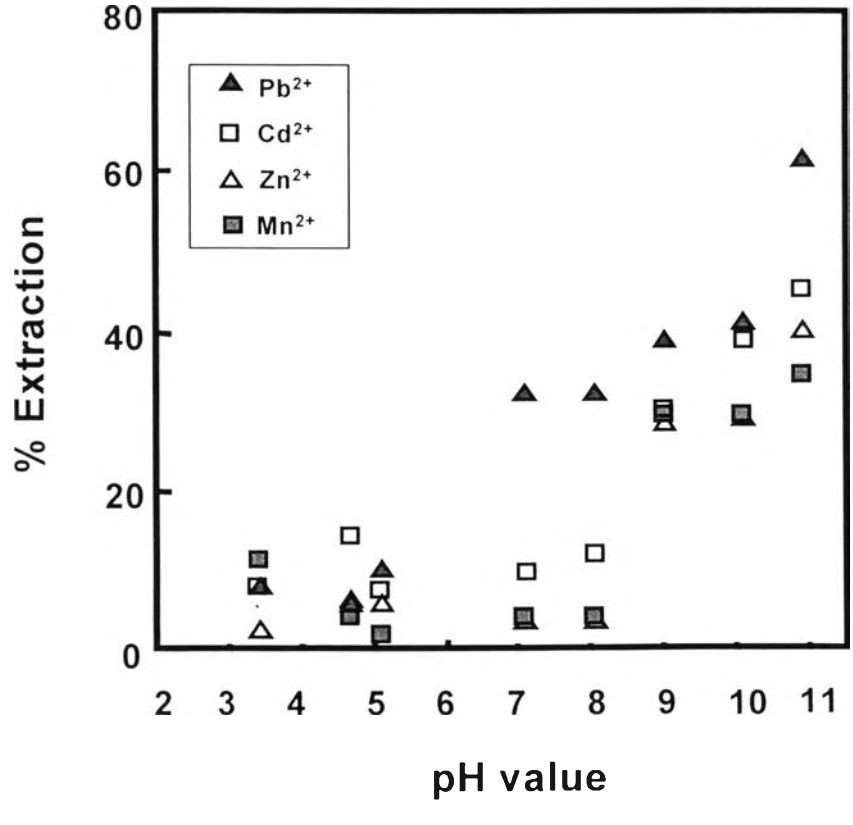

Figure 4.9 Percent extraction of **3** in various pH values.